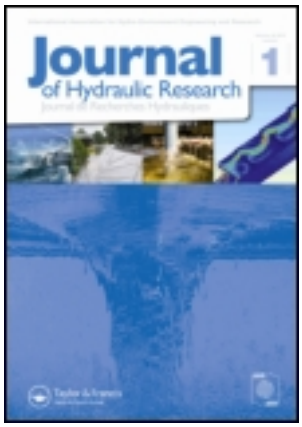

Journal of Hydraulic Research
Publication details, including instructions for authors and subscription information:
http://www.tandfonline.com/loi/tjhr20

Multi-frequency acoustics for suspended sediment studies: an application in the Parana River

Massimo Guerrero (IAHR MEMBER), Laboratory Engineer[a], Ricardo N. Szupiany Associate Professor[b] & Francisco Latosinski PhD Student[c]

[a] Hydraulic Engineering Laboratory, University of Bologna, Via Terracini, 40131 Bologna, Italy

[b] Faculty of Engineering and Water Sciences, International Centre for Large River Research (CIEGRI), Littoral National University, Santa Fe City, Santa Fe, CP 3000, CC 217, Argentina Email:

[c] Faculty of Engineering and Water Sciences, International Centre for Large River Research (CIEGRI), Littoral National University, Santa Fe City, Santa Fe, CP 3000, CC 217, Argentina Email:

Published online: 31 Oct 2013.

To cite this article: Massimo Guerrero (IAHR MEMBER), Laboratory Engineer, Ricardo N. Szupiany Associate Professor & Francisco Latosinski PhD Student (2013) Multi-frequency acoustics for suspended sediment studies: an application in the Parana River, Journal of Hydraulic Research, 51:6, 696-707, DOI: 10.1080/00221686.2013.849296

To link to this article: http://dx.doi.org/10.1080/00221686.2013.849296

Journal of Hydraulic Research Vol. 51, No. 6 (2013), pp. 696–707
http://dx.doi.org/10.1080/00221686.2013.849296

Research paper

Multi-frequency acoustics for suspended sediment studies: an application in the Parana River

MASSIMO GUERRERO (IAHR MEMBER), Laboratory Engineer, *Hydraulic Engineering Laboratory, University of Bologna, Via Terracini, 40131 Bologna, Italy*
Email: massimo.guerrero@unibo.it (author for correspondence)

RICARDO N. SZUPIANY, Associate Professor, *Faculty of Engineering and Water Sciences, International Centre for Large River Research (CIEGRI), Littoral National University, Santa Fe City, Santa Fe, CP 3000, CC 217, Argentina*
Email: rszupiany@yahoo.com.ar

FRANCISCO LATOSINSKI, PhD Student, *Faculty of Engineering and Water Sciences, International Centre for Large River Research (CIEGRI), Littoral National University, Santa Fe City, Santa Fe, CP 3000, CC 217, Argentina*
Email: franlatos@gmail.com

ABSTRACT
A method of using two acoustic Doppler current profilers operating at different frequencies and employed at the same measuring vertical to sample a profile of suspended sediment concentration has been previously applied in the Parana River (Argentina) but has not been validated by direct sediment samples. The present work fills this gap by reporting new field data and comparing them with acoustically inferred sediment concentrations. The agreement between directly measured sediment concentrations and grain sizes with corresponding estimates from an employed backscatter model was found to be good (squared correlation coefficients are 0.9 and 0.8, and mean deviations are 14 and 6%, respectively). The interrelations between flow velocity and suspended sediment concentration at fixed locations and in a moving mode along a river cross-section have been also investigated. Observed events of bed sediment re-suspension were found to be highly correlated with fluctuations of the vertical flow velocity, with a 100–150s quasi-periodicity. The size of re-suspension plumes was increasing from the channel thalweg to the low-submerged bar areas.

Keywords: ADCP; backscatter; bed sediments; field studies; multi-frequency; Parana River; suspended sediments

1 Introduction

Standard suspended sediment measuring procedures for large channels require multi-point or depth-integrating sampling at multiple locations across the channel. These methods are usually time-consuming, expensive, labour-intensive, and typically have limited spatial and time resolutions. Therefore, the possibility of indirectly quantifying suspended sediments by non-intrusive instruments using ultrasound echoes has been widely investigated since the beginning of the 1980s (Hay 1983, Hay and Sheng 1992, Holdaway *et al.* 1999, Creed *et al.* 2001, Thorne and Hanes 2002, Filizola and Guyot 2004, Hoitink and Hoekstra 2005, Kostaschuk *et al.* 2005, Guerrero *et al.* 2011).

The most promising method is based on the principle of a frequency-dependent variation in the backscatter of particles and applies when the product of the acoustic wave number and grain radius is less than one. This approach, known as the multi-frequency method, was first tested by Hay and Sheng (1992). Thorne and Hanes (2002) demonstrated the ability of a multi-frequency acoustic backscatter (ABS) instrument to measure both sediment concentrations and grain size profiles near sea-beds, typically down to 1 m above the bed. Thorne and Hanes (2002) also presented results from laboratory experiments that allowed to quantify the form function (characterizing scattering properties of a particle) and the normalized total scattering cross-section of irregularly shaped particles.

In the river environment, experiments to measure sediment concentrations together with grain size profiles using a moving vessel equipped with 1200- and 600-kHz acoustic Doppler current profilers (ADCPs) were performed in the Po River (Italy) by Guerrero and Lamberti (2008) and in the Parana River (Argentina) by Guerrero *et al.* (2011). In particular, Guerrero

Received 24 October 2012; accepted 24 September 2013/Open for discussion until 30 June 2014.

ISSN 0022-1686 print/ISSN 1814-2079 online
http://www.tandfonline.com

and Lamberti (2008) demonstrated that it is possible to assess both the concentration and grain size maps using two ADCPs deployed at the same measuring vertical and operating in a multi-frequency regime. The resulting maps were applied in a hydro-morphodynamic model validation in Guerrero *et al.* (2013). Single- and multi-frequency ADCP methods are compared in Guerrero *et al.* (2011). The former is widely accepted as a reliable method to characterize the distribution of suspended sediment concentration, although this method neglects the effect of grain size on the scatter. The multi-frequency technique is a more advanced method that provides both the concentration distribution of suspended sediments and the grain size profiles by incorporating the effect of grain size on the scattering process. In Guerrero *et al.* (2012), multi-frequency method was validated in laboratory by acoustically profiling the same water column with beams of two different frequencies (600 and 1200 kHz ADCPs) under controlled conditions for suspended sediment concentrations and grain sizes.

Despite the advances made in recent studies, the multi-frequency method using ADCP has not yet been verified in a large river using directly measured grain sizes and concentrations from water samples. In this study, the multi-frequency technique based on two ADCPs operating at 600 and 1200 kHz, which are deployed at the same location to measure profiles of the suspended sediment concentrations and grain sizes, is tested against sampled concentrations and grain size distributions in the Parana River. Furthermore, measurements at separate locations and at a cross-section of the Parana River provide examples demonstrating the improved capabilities of standard ADCPs for investigating river processes.

This paper is based on a field survey performed at the Parana River bifurcation near Rosario City, Argentina. The experimental site and procedures are described first. Measurements included simultaneous ADCP profiling and water sampling at four fixed locations (two within the main channel and two within a secondary reach), and a moving ADCP profiling across the river channel upstream of the bifurcation. Next, the multi-frequency ABS method is briefly summarized, focusing on the calibration of the ADCP echo intensities using concentrations and grain sizes from the water samples. The results are then presented in relation to (1) sediment characterization from the samples; (2) validation of the dual-ADCP method against sediment samples and flow/sediment profiles at fixed locations; and (3) comprehensive investigation of the concentrations, grain sizes and velocity fields along a river cross-section, as an illustration of the method's application and its effectiveness in enhancing ADCP capabilities. Finally, the method's limitations are discussed in the context of the results and existing technologies. The method's advantages in studies of sediment transport mechanisms are also highlighted.

2 Study Site and Methods

2.1 *Study site and field measurements*

The Parana River is one of the largest rivers in the world (Latrubesse 2008), with a drainage basin of 2.3×10^6 km^2 crossing the borders of Brazil, Bolivia, Paraguay and Argentina. Downstream of the confluence of the Parana River and the Paraguay River (Fig. 1), the mean annual discharge is 19,500 m^3 s^{-1} and the water surface slope is of the order of 10^{-5}. The channel bed is composed mostly of fine- and medium-sized sand (Drago and Amsler 1998). The channel planform pattern can be classified as anabranching with a meandering thalweg (Latrubesse 2008). A succession of wider and narrower sections is typical, with mean channel widths and depths ranging from 600 to 2500 m and from 5 to 16 m, respectively. The study site is located in the lower part of the Parana River near the city of Rosario (Fig. 1) and represents a large expansion–bifurcation unit. The site was surveyed on 16 and 17 November 2010 when the total flow discharge was 14,320 m^3 s^{-1}.

Bed and suspended sediment samples were obtained at four fixed measuring verticals (P1, P2, P3 and P4 in Fig. 1) positioned across the river cross-section upstream of the bifurcation. Two Teledyne-RDI (San Diego, CA, USA) ADCPs operating at frequencies of 600 and 1200 kHz were simultaneously used for

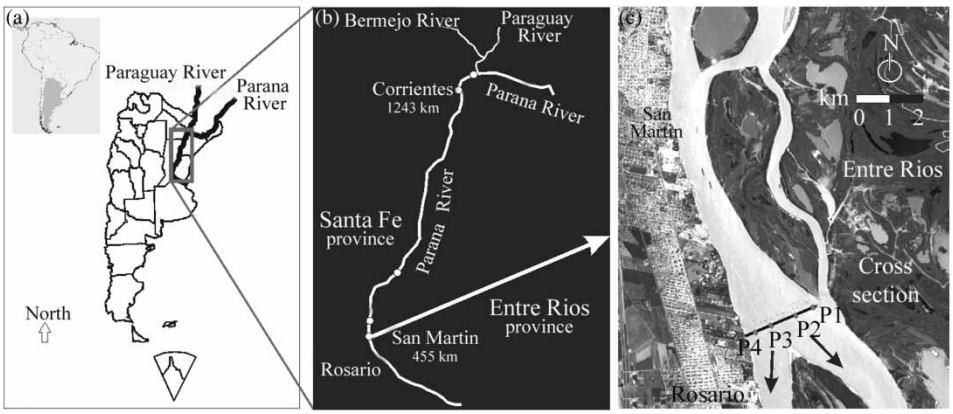

Figure 1 (a and b) Study site of the Parana River; (c) measurement cross-section and fixed locations P1, P2, P3 and P4

profiling water columns. At each measuring vertical, 2–3 suspended sediment samples were collected with a depth-integrating isokinetic sampler to reduce the effect of temporal fluctuations in the resulting sediment concentrations (Garcia 2008). Also, one bed sample was collected at each location. The concurrent echo intensities for the two applied frequencies were then calibrated against the backscatters predicted for the depth-integrated suspended sediment samples, and the corresponding differences between backscatters at the two frequencies were used to validate the ADCPs' methods for grain sizes assessment. The same ADCPs were used to quantify the temporal variability of the flow velocity, suspended sediment concentration and grain size at the locations P1, P2, P3 and P4 as well as the distributions of these parameters along the river cross-section (Fig. 1) obtained in a moving mode repeated four times. The horizontal positions were provided with an accuracy of ± 0.02 m at the update frequency of approximately 1 Hz by surveying in real-time kinematic mode with the differential global position system. The ADCPs were operated following the standard principles and restrictions of Doppler profilers, which can be found in Gordon (1996), Muste *et al.* (2004a, 2004b), Oberg *et al.* (2005), Szupiany *et al.* (2007b), and Guerrero and Lamberti (2011).

The suspended sediment samples were analysed involving the following steps: (1) sand separation from finer sediments, i.e. silt and clay, by means of wet sieving; (2) computation of the sediment concentrations and (3) assessment of the grain size distribution of the suspended sand particles with a scanning electron microscope.

2.2 *Acoustic methodology*

The multi-frequency method for profiling concentration and size of sand was reported by Hay and Sheng (1992), and therefore here only the basic information relevant to this study is given. The method is found on the basic principles of the active-sonar that is a sound source that produces a sound level (namely, SL) and also acts as a receiver. When the radiated sound reaches a target (e.g. sediment particles) and travels back towards the source, its level will be reduced by the transmission losses (2TL for back and for) and enhanced on reflection or scattering by the target strength (TS that is the backscattering power). Therefore, the received echo level (RL) measured by the sonar can be expressed by the basic equality (Eq. 1) between the logarithmic levels of sound:

$$\mathrm{RL} = \mathrm{SL} - 2\mathrm{TL} + \mathrm{TS} \tag{1}$$

that is the active-sonar equation (Urick 1997, Medwin and Clay 1998). This equality is particularly relevant when using an ADCP because each of its transducer is an active-sonar that records the received echo in a logarithmic scale. Therefore, the TS may be assessed on the basis of Eq. (1). However, the active-sonar equation was recast in the working form reported in Eq. (2) that was adopted in the design of the Teledyne-RDI ADCPs (Denies 1999). Given the instrument parameters and record, Eq. (2) yields the backscattering power (i.e. TS) for unit volume in decibel scale (dB).

Table 1 Symbol correspondence between the active-sonar equation (Eq. 1) and its working form (Eq. 2) for the ADCP

Equation (1)	Equation (2)
TS	S_v (backscattering power)
RL	$C + K_c(E - E_r)$ (calibrated intensity of the effective-echo level)
2TL	$10\log_{10}(T + 273.16)R^2 + 2\alpha R$ (sound spreading and absorption)
SL	$L + P$ (transmitted pulse length and power)

$$S_v = C + 10\log_{10}(T + 273.16)R^2 - L - P + 2\alpha R + K_c(E - E_r) \tag{2}$$

The meaning of symbols and quantities in Eq. (2) can be retrieved from Eq. (1) as it is described in Table 1. In more detail, the coefficient C (in dB) is calibrated to relate the measured echo intensity E to the modelled backscattering power S_v from suspended sediment. The parameters T and R are the transducer temperature in °C and the acoustic beam range in metres, respectively (from ADCP raw data). The parameters L and P are 10 times the common logarithm of the transmitted pulse length (in m) and the transmitted power (in W), respectively (also from ADCP raw data). The coefficient α (in dB/m) accounts for sound absorption and is modelled following Medwin and Clay's (1998) formulation for water viscosity attenuation.

The sound losses due to the presence of suspended sediment are the sum of two terms: (1) viscous dissipation due to the relative motion between sediment particles and water; and (2) sound scattering by particles. Various formulations can be found in the literature to assess these losses; among others, Hanes (2012) reported a comparison between the two terms as a function of sediment size and applied frequency, showing a negative correlation between scattering and viscous dissipations. Sound losses due to viscous stresses are dominant for silt and clay, whereas scattering losses prevail in the sand range. In both cases, sound losses increase with its frequency. In the Parana River case study, the formulations by Urick (1948) and Thorne and Hanes (2002) for viscous and scattering dissipations, respectively, were applied, yielding low values compared with the corresponding backscattering power. The total attenuation due to the suspended sediment was mostly related to the fine-sediments (i.e. diameter 5–10 μm and concentration of 90 μg/l) and at its maximum was only a few percent of the assessed scattering power. The sound losses due to scattering were on the order of 10^{-3} of the viscous dissipation and were negligible in the investigated section of the Parana River (Guerrero *et al.* 2011).

The conversion factor K_c for the echo intensity (into dB) in Eq. (2) was obtained by means of a laboratory test using an hydrophone (RD Instruments 1999). The parameter E is the ADCP-measured echo intensity in counts and E_r is the echo

intensity corresponding to the ambient noise level which is typically obtained from the ADCP-measured echo intensity at the largest distance from transducers.

The mass of suspended sediments per unit volume, i.e. the concentration M, is related to the backscattering power as (Thorne and Hanes 2002)

$$M = \frac{s}{\sigma}\rho_s \frac{4}{3}\pi a^3 \tag{3}$$

where a is the particle radius (particles are assumed to be spherical), ρ_s is the particle density and the ratio s/σ gives the number of particles for unit volume. s is the backscattering power related to S_v as

$$s = 4\pi\, 10^{S_v/10} \tag{4}$$

σ is the backscattering power for an average single particle within the measurement volume (namely, scattering size). The scattering size was related to the physical size by the form factor f according to Thorne and Hanes (2002)

$$\sigma = \frac{2}{3}a^2 f^2 \tag{5}$$

where the form factor is a function of ka, which is the acoustical wave number–particle radius product. The form factor function of ka is reported in Thorne and Hansen (2002), among others. The concentration expressions for the two frequencies (Eq. 3) yield the relationship to solve for grain size (Eq. 6):

$$\frac{s_1}{\sigma_1} = \frac{s_2}{\sigma_2} \tag{6}$$

where the subscripts refer to the applied frequencies. Equation (6), which is not dependent on concentration, gives the current mean grain size of an ensonified volume by the two frequencies. By substituting σ with its expression (Eq. 5), Eq. (6) is recast to determine the grain size from the backscattering power ratio at two frequencies

$$\left(\frac{f_1}{f_2}\right)^2 = \frac{s_1}{s_2} \tag{7}$$

or from their difference in dB

$$10\log_{10}\left(\frac{f_1}{f_2}\right)^2 = S_{v1} - S_{v2} \tag{8}$$

The form factors square ratio (in the left-hand side of Eqs. 7 and 8) is a function of the sediment grain size and the applied frequencies through the ka product as reported in Hay and Sheng (1992). An advantage of this method is its ability to estimate the mean grain size in the ensonified volume.

The ADCP-measured echo intensity was related to the backscattering power that, in turn, was modelled on the basis of the sampled concentrations and grain sizes. For this purpose, the working form of the sonar equation was recast in the following form (Eq. 9):

$$S_v - S_c = C + K_c(E - E_r) \tag{9}$$

This form better shows the calibration parameters: C and K_c, which are the intercept and slope coefficients, respectively, for the applied linear fitting. In Eq. (9), S_c (namely, the backscattering power correction) includes all of the known terms of Eq. (2); $(E - E_r)$ is the measured effective echo intensity which also accounts for echo intensity corresponding to the ambient noise level; and S_v is the backscattering power determined by Eq. (10), which is derived from the assumed scattering model for sand (Eqs. 3–5)

$$S_v = 10\log_{10}\frac{Mf^2}{8\pi^2\rho_s a} \tag{10}$$

where M and a are the concentration and the particle radius (derived from the samples), respectively.

The interpretation of the backscattering power from suspended sediment and how to extract sediment features (i.e. concentration and size) from a backscatter signal are referred to in the literature as forward and inverse problems, respectively. The performed calibration implied a forward problem, i.e. given the sediment features from samples, the backscattering power was predicted (by Eq. 10) and was then related (by Eq. 9) to the echo intensity measured during sampling. The calibrated method was then applied to the entire record obtained from both ADCPs, thus extracting the variation in the suspended sediment features from the backscatter signal estimated at some river locations, which is of major interest for hydraulic-sediment studies. Therefore, given the measured echo intensity, the inverse problem consisted of assessing the backscattering power using Eq. (9) for application in Eqs. (10) and (8), which yielded the actual concentration and grain size, respectively, at each measurement cell.

Regarding the inverse problem, the sediment grain size can be derived from the difference between backscattering powers at different frequencies within a limited range of ka; in fact, for $ka \ll 1$ and $ka \gg 1$, there is no size information in Eq. (8) (Thorne and Hansen 2002). In addition, a ka value near 1 may lead to multiple grain size values (Thorne and Hardcastle 1997), and the backscatter signal below the instrument and ambient noise levels further reduces the method applicability for low ka values.

3 Results

3.1 *Sediment samples*

Observed distributions of sand from the river-bed and water columns were averaged over three samples in P1, P2 and P3 and two in P4 (Fig. 2), the complete data set is reported in Table 2. It is worth noting that bed and suspended sand sizes are not evenly distributed along the river cross-section. This was observed in the median grain size sampled. The median grain sizes D_{50} from

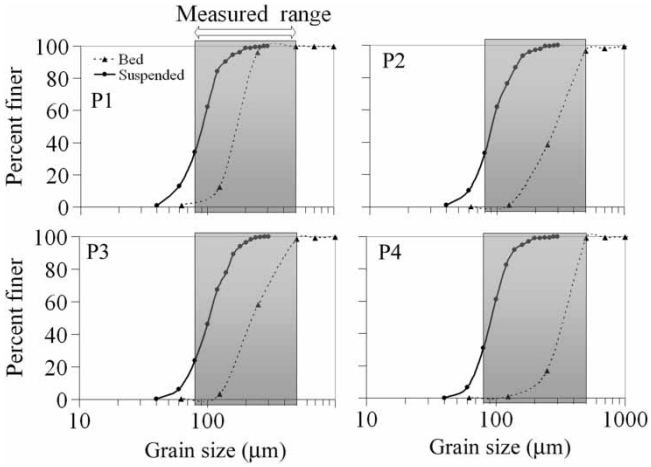

Figure 2 Average distributions of grain size of bed and suspended sand in P1, P2, P3 and P4 over the acoustically measured range

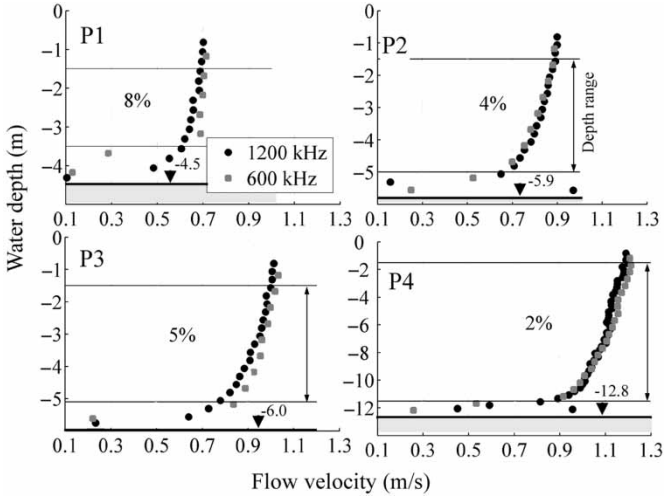

Figure 3 Time-averaged profiles of flow velocity (at fixed locations P1, P2, P3 and P4) measured by the two ADCPs with the indication in percent of their deviation from each other within the depth range for the acoustic method application

the river-bed were 170, 280, 210 and 340 μm in P1, P2, P3 and P4, respectively (maximum value in P4 and minimum in P1), whereas for the suspended sand, D_{50} were 91, 94, 111 and 92 μm (maximum in P3 and minimum in P1) in the same positions. This misalignment gave evidence on a different variation along the cross-section for bed and suspended sand which was also discussed in more detail by Szupiany *et al.* (2012).

The amount of particulate organic matter is negligible in the main channel of the Parana River, with concentrations lower than 0.1 mg/l which does not appreciably affect the backscattering power (Szupiany *et al.* 2009). The effects by silt and clay on sound propagation were also neglected, fine sediment was within the range of 5–10 μm and almost homogenously distributed across the channel width (mean values are 86, 81, 88 and 93 mg/l in P1, P2, P3 and P4, respectively). Additionally, fine sediment does not flocculate in the Parana River's channel because of high flow velocities (Mangini *et al.* 2003).

3.2 *Validation of the dual-ADCP method at fixed vertical sections*

The depth ranges (Fig. 3) for the application of the acoustic method were critically investigated to account for (1) the backscattering power in the near field is strongly affected by instrumental noise and (2) close to the river-bed, the side lobes interference, the hard boundary reflection and the horizontal separation resulting from the diverging beams combine to produce measured echo intensities that are no longer related to the scattering from suspended sediment. In addition, the velocity profiles measured by the two ADCPs were compared to verify the homogeneity of the water volume to which the acoustic calibration was applied.

Velocity profiles (measured from the two ADCPs) were averaged (Fig. 3) over water sampling intervals. A noticeable gradient in the averaged profiles near the river-bed confirms that the backscatter values in this region are likely uncorrelated to suspended sediment but are affected by the near boundary (e.g. bed-load scatter). In addition, in several cases, the echo levels were not available in the deepest bins, which occurred due to the acoustic beams ensonified different depths close to the river-bed because of the local morphology (e.g. bar and bed slope). At these conditions, beam spreading and divergence may lead to side lobe interference (Gordon 1996) and measurements of different sediment fluxes by the two ADCPs. These occurrences

Table 2 Data from suspended sand samples and the ADCPs record in P2, P3 and P4

	Samples				1200-kHz ADCP		600-kHz ADCP		Comparison domain for ADCP echo intensities	
Position and sample #	M (mg/l)	D_{50} (μm)	D_{84} (μm)	D_{16} (μm)	$S_v - S_c$ (dB)	$E - E_r$ (count)	$S_v - S_c$ (dB)	$E - E_r$ (count)	Average time (min)	Range (m)
P21	15.7	96	123	68	−84.3	125.9	−90.7	149.5	6	1.5–5.0
P22	20.0	89	122	67	−84.3	126.1	−90.5	149.9	5	
P23	15.7	97	135	72	−84.2	126.2	−90.7	149.5	4	
P31	29.3	120	162	85	−83.3	128.6	−89.0	153.3	3	1.5–5.1
P32	29.2	122	148	84	−82.7	129.9	−88.4	154.7	3	
P33	32.4	90	115	73	−82.7	130.0	−88.6	154.2	3	
P41	16.1	88	122	72	−92.7	104.9	−97.7	133.4	4	1.5–11.5
P42	16.7	98	146	76	−92.2	106.2	−97.2	134.6	3	

strongly affect the method applicability, as is the case for the P1 position. The time averaged profiles in P1 deviated more than 5% from each other within the candidate depth range (percent deviation in Fig. 3), providing evidence of a lack of horizontal homogeneity of the flow field within the whole control volume of the two ADCPs. This lack of horizontal homogeneity is likely a result of the river channel shape. Position P1 was therefore discarded in the following analyses because the ensonified volumes (corresponding to sampling column) cannot be assumed to be equal for the two frequencies. No significant deviations arose within the depth ranges of sampling in P2, P3 and P4 positions, as seen from the corresponding velocity profiles and percent deviations in Fig. 3. The P2 position was near the centre of the streamflow for the secondary channel, and the other two positions were in the streamflow of the main channel (see Figs. 1 and 8 for the locations on the river map and within the surveyed cross-section, respectively).

Depth-averages of ADCPs profiles were time-averaged over the water sampling intervals (e.g. boxes in Fig. 4a–c), equal to approximately 200 s, to compare with the depth-integrated samples. This averaging time yielded time-averaged echo intensities and velocities pretty close to the corresponding long-term averages (Szupiany *et al.* 2007a) as can be inferred from the variability in the averaging time, t, of the normalized mean deviations (NMs) (Fig. 4b–d). The NM is defined as the ratio of the actual cumulative mean minus the entire time series mean over the entire time series mean (Guerrero and Lamberti 2011), as described by Eq. (11) for echo intensity

$$\mathrm{NM} = \frac{\overline{E_0^t} - \overline{E}}{\overline{E}} \tag{11}$$

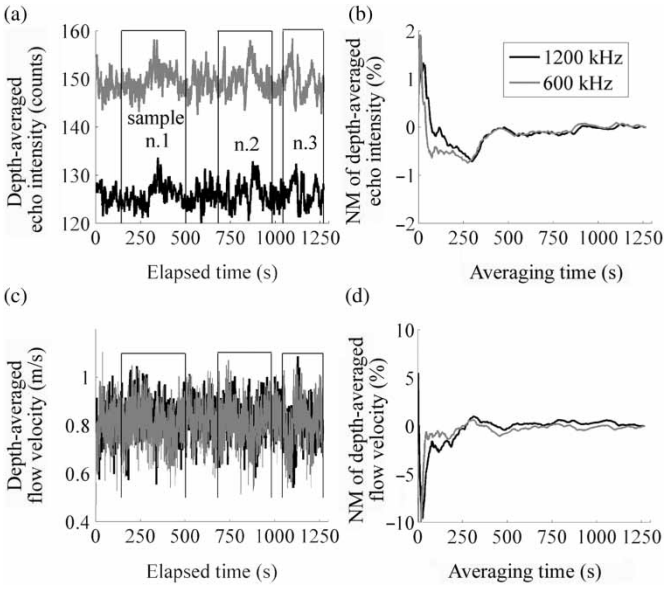

Figure 4 (a) Time series of depth-averaged intensities of effective echoes at P2; (b) NMs of depth-averaged intensities of effective echoes at P2; (c) time series of depth-averaged flow velocities at P2 and (d) NMs of depth-averaged flow velocities at P2

A qualitative correlation was observed between the NMs of the depth-averaged velocity and the NMs of the echo intensities that may reflect the flow velocity-suspended load reciprocal influence. Thus, the depth-averaged echo intensities from the ADCPs were time-averaged over the sampling times, and the resulting values were applied in Eq. (9) to match the backscattering power values estimated by means of Eq. (10) on the basis of sampled concentrations and grain sizes in P2, P3 and P4 (i.e. forward problem). The ADCPs and samples data are summarized in Table 2. At the end, a total of eight ADCP record-sample pairs were available: three in P2, three in P3 and two in P4.

Using the 1200- and 600-kHz ADCPs, laboratory tests performed by Guerrero *et al.* (2012) were successful in sizing the particle diameters in the range of 100–600 μm, which roughly correspond to an acoustical wave number–particle radius product, ka, within the range of 0.20–1.00. In those tests, the size range was also limited by the noise level of air bubbles introduced in the laboratory facility, which covered, to some degree, the scattering power of the finer sediment. Given this evidence, sizes finer than 80 μm were discarded from the sampling results to estimate the backscattering power. Therefore, the median radii of sediment fractions coarser than 80 μm (from the suspended sediment samples) were applied in Eq. (10), which roughly corresponded to the D_{80} of each sample. Consequently, in Eq. (10), the observed concentrations (M in Table 2) were systematically reduced by 20%. In other words, in the Parana case study, using the echo intensities from the 1200- and 600-kHz ADCPs, the acoustically investigated range of suspended sediment had a lower bound of 80 μm (see the measured range in Fig. 2).

The parameters K_c and C (for the 1200- and 600-kHz ADCPs) were inferred from the calibration (least squares algorithm) of Eq. (9) over the experimental data (Fig. 5), where S_v was modelled by Eq. (10) and E was from the ADCP echo intensity profiles. Squared correlations between the acoustically inferred and the reduced concentrations from the samples resulted in values of 0.6 and 0.9 for the samples set and mean values at fixed positions, respectively. The corresponding squared correlation for grain sizes were 0.5 and 0.8, respectively. The terms used

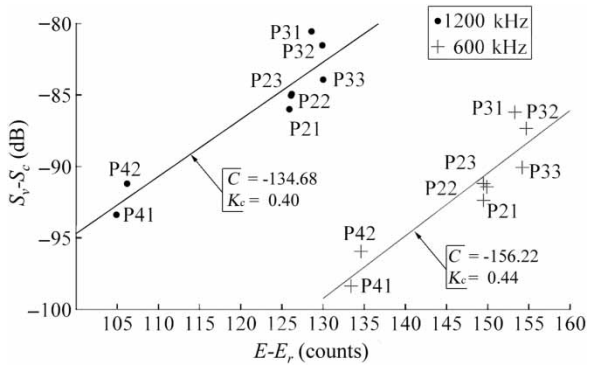

Figure 5 Calibrated linear relations between effective echo intensity (measured $E - E_r$) and corrected scattering power (modelled $S_v - S_c$) with corresponding coefficients (C and K_c) for 600- and 1200-kHz ADCPs

Table 3 Theoretical (second column) and field evaluated (third column) ratios of scattering powers from two acoustic frequencies (1200 and 600 Hz) and corresponding results in terms of sediment concentrations and grain sizes

Position and sample #	$\left(\frac{f_{1200}}{f_{600}}\right)^2$	$\frac{s_{1200}}{s_{600}}$	Acoustically inferred concentration (mg/l) and corresponding absolute deviation in % from samples				Acoustically inferred grain size (μm) and corresponding absolute deviation in % from samples			
P21	14.1	13.9	19	47%	18	27%	127	3%	126	1%
P22	14.1	13.6	20	21%			136	11%		
P23	13.7	14.3	15	15%			114	16%		
P31	12.8	13.1	13	47%	23	10%	154	5%	152	7%
P32	13.3	12.8	19	23%			162	9%		
P33	14.3	13.6	37	36%			139	21%		
P41	14.1	14.1	16	16%	13	4%	120	2%	121	10%
P42	13.3	14.1	11	23%			121	17%		

in Eq. (7), the resulting grain sizes and concentrations for each sample, and the average values at sampling positions are reported in Table 3. The corresponding absolute deviations from the samples (reduced values, i.e. D_{80} and $0.8M$) are listed in the same table. The mean deviations were approximately 29 and 11% for the concentration and grain size, respectively, and approximately half of those values are from the average values at the sampling positions.

The calibrated method was then applied to the entire ADCPs record, thus characterizing the time and depth variation in the suspended sediment (i.e. inverse problem) at the three fixed locations. In this case, the applied averaging to ADCPs record defined the resulting time resolution. The 1200- and 600-kHz water pings were spaced 0.09 and 0.20 s apart, respectively (i.e. the time between pings was equal to 0.09 and 0.20 s), and were grouped in 0.5 and 0.6 s ensembles during deployment, i.e. 5 and 3 pings for each ensemble. The individual velocity and echo intensity profiles were grouped and averaged on a 3-s time basis, reducing the eventual time misalignment between the ensembles (measured profiles) from the two instruments. In addition, aiming to further reduce the resulting variability, following the calculation of the concentration and grain size, boxcar averaging was performed along a 15-s spaced grid, including five resulting profiles in each mesh. A linear interpolation with a fixed step of 0.2 m was also applied to evenly distribute the bins along the vertical profiling,

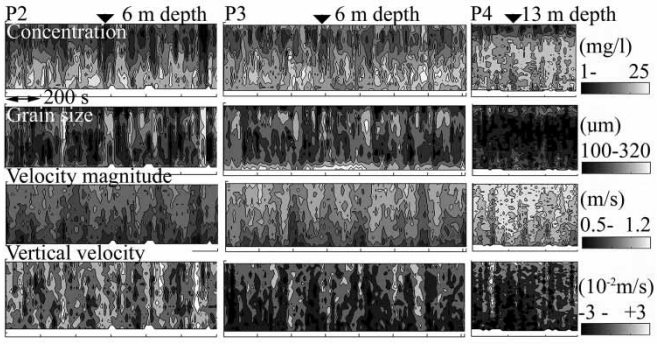

Figure 6 Profile time series of sediment concentration, grain size and corresponding velocity magnitude and vertical velocity (upward positive values) at fixed positions (P2, P3 and P4)

thus compensating for the misalignments between the measurement bins of the two acoustic frequencies; in this case, they were 0.25 and 0.5 m for the 1200- and 600-kHz ADCPs, respectively.

The resulting time series present vertically aligned contours (Fig. 6) in the three fixed positions (P2, P3 and P4), which are possibly related to periodic events of sediment re-suspension from the river-bed towards the water surface. These typical patterns were correlated among different variables (i.e. concentration, grain size, velocity magnitude and vertical velocity) and presented the clearest periodicity at approximately 100–150 s, albeit lower variations were also observed at higher frequencies (with 40–60 s as the time period). In addition, a similar periodicity was observed for the depth-averaged velocity and echo intensity at all the fixed positions (Fig. 4). Positive correlations were observed between the concentration and velocity magnitude and between the grain size and vertical velocity, whereas the sediment concentration and grain size were negatively correlated. In other words, on average, low concentrations of coarse sediment corresponded to upward fluxes, whereas finer sediment was observed in the zone with higher velocity magnitude (P4). In the low-water-depth profiles (P2 and P3), the vertically aligned patterns were particularly evident. These results provide evidence on two different mechanisms for coarse and fine sediments: (1) the coarse sediment entrainment from the bed into the stream flow occurs by means of vertical advection in secondary currents (at low depths: P2 and P3); and (2) the transport of fine sediment in the core of the main streamflow (P4) is characterized by high velocities.

3.3 *River cross-section survey*

To show the effectiveness of the calibrated method in enhancing ADCP capabilities for fluvial process investigations, the river cross-section in Fig. 1 was surveyed with the instrument typical deployment used for streamflow discharge measurement and velocity field mapping (Szupiany *et al.* 2007a, Guerrero and Lamberti 2011). The two calibrated ADCPs were moved along the river cross-section as the echo intensity and velocity profiles were continuously measured.

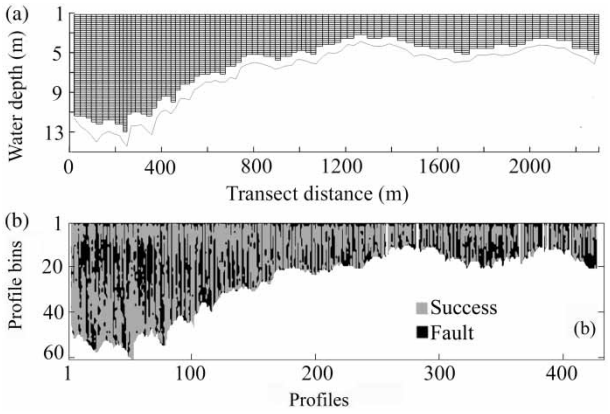

Figure 7 (a) Data grid for profiles averaging and (b) proxy indexes of success in individual bins of the two-ADCP method

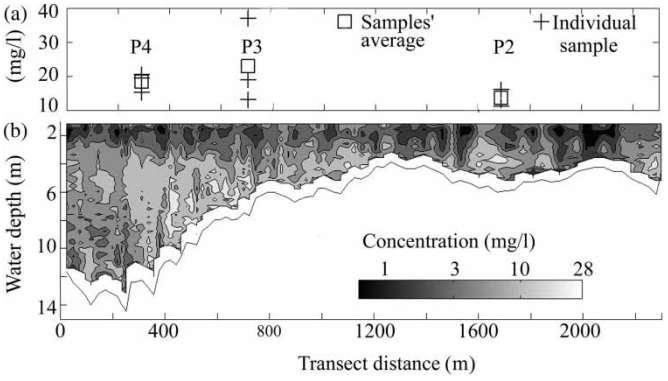

Figure 8 (a) Concentration values from the acoustic method corresponding to the samples' average and to individual samples over transect distance and (b) acoustically inferred map of concentration along the investigated cross-section, transect distance from the right bank

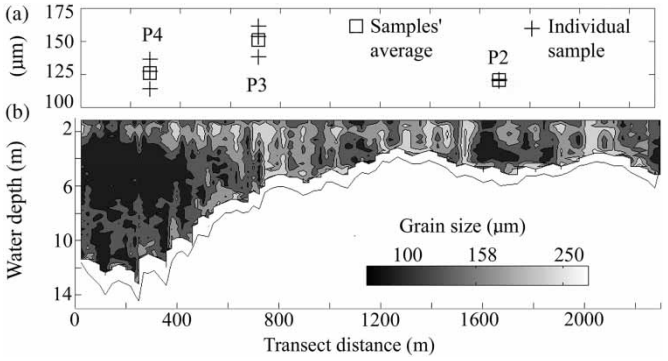

Figure 9 (a) Sediment size values from the acoustic method corresponding to the samples' average and to individual samples over transect distance and (b) acoustically inferred map of sediment size along the investigated cross-section, transect distance from the right bank

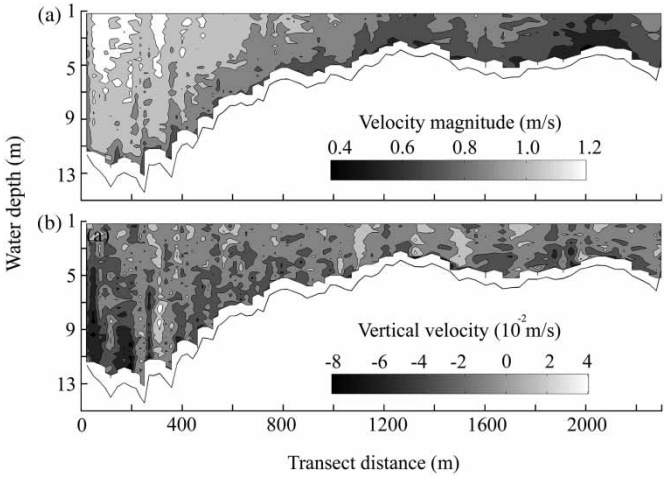

Figure 10 (a) Velocity magnitude map from 1200-kHz ADCP and (b) vertical velocity map from 1200-kHz ADCP, upward positive values, transect distance from right bank

Analogous to the previously described analysis for the fixed positions, the moving-ADCPs profiles were averaged to achieve reliable time and vertical alignments between the two instruments. Individual ensembles (measured profiles) were averaged together on a 3-s time interval. Following the inverse problem solution, 15-s boxcar averaging was performed on the resulting profiles, the same as in the case of the analysis at fixed positions. Although, the method application to individual bins was limited by (1) side lobes interference close to the river-bed; (2) the diverging beams configuration and (3) the *ka* range; boxcar averaging led to concentration and grain size estimates for the entire section. Given the fixed interval for averaging, lower boat velocities resulted in a finer mesh for the post-processing grid (Fig. 7a). The final resolution along the cross-section was approximately 30 m on average, 20 m at the minimum and twice that at the maximum, which is sufficient for the investigated 2.3-km wide cross-section. A linear interpolation with a 0.2-m step was also applied to distribute the bins evenly along the vertical axis.

Deviations between the averaged profiles of the flow velocity magnitude from the two ADCPs, referenced to a bottom track option (Gordon 1996), were randomly distributed along the cross-section, and the mean and maximum values were 5 and 10%, respectively, providing evidence on the successful alignment of the acoustic beams and supporting the assumption of layer homogeneity within the two ADCP measurement volumes. Success and fault in applying the dual-ADCP method at an individual bin are mapped in Fig. 7b. Method faults were due to the following factors: (1) ADCP profiling limitations (e.g. the unmeasured regions near the instruments and river-bed); (2) different ensonified volumes for the two ADCPs (i.e. the lack of horizontal homogeneity in the investigated water volume) and (3) values of *ka* being too low which was particularly frequent at the streamflow core (profiles between 1 and 75 in Fig. 7b).

As expected, a good agreement was observed between the variation of the variables along the cross-section derived from the moving- and fixed-deployment (Figs. 8 and 9). A high-concentration pattern can be observed beginning from the river-bed (Fig. 8) where coarse sediments were also observed (Fig. 9), which provided evidence on sediment entrainment into the streamflow from the bed. In more detail, sand plumes, characterized by the highest concentrations (within the range of

10–20 mg/l) found in the cross-section, were observed at the main channel side (transect distances between 300–1200 m from the right bank in Fig. 8). These vertical plumes were correlated with vertical velocity variations that were particularly evident from a transect distance between 300 and 600 m (Fig. 10b) and corresponded to the vertically aligned patterns in the velocity magnitude field (Fig. 10a). The corresponding grain sizes (Fig. 9) decreased, passing from 150–200 μm in low-depth areas to approximately 100 μm for plumes near the stream flow channel (high water depth). Low concentrations (3–10 mg/l) of fine sediment (90–100 μm) were observed in the streamflow core (Figs. 8 and 9): within 0–400 m and 12–8 m for the transect distance and water depth, respectively.

4 Discussion

The dual-ADCP method requires that an almost homogenous volume be simultaneously ensonified by different frequency beams. Additionally, the profiled water columns were simultaneously sampled for method validation purposes. Taking into account the existing ADCPs and the difficulties of field operations on a large, navigable way, such as the Parana River, the time-spatial alignment task was not trivial for the following reasons: (1) the different time and profile resolutions of the ADCPs and water sampler; (2) the diverging beam configuration of the ADCPs and the use of two instruments, which further increased the ensonified volume and thus, the extent of the layer homogeneity assumption and (3) the different time and profile resolutions of the 1200- and 600-kHz ADCPs, which in this study, corresponded to ping intervals of 0.09–0.20 s, respectively. The first constraint forced the validation to be conducted on depth- and time-averaged values. However, the second and third constraints also play relevant roles, particularly where the velocity field presents noticeable gradients in the horizontal plane, as was the case of position P1.

When using two ADCPs working at different frequencies for combined concentration–grain size mapping, the typical assumption of layer homogeneity (Gordon 1996) in the horizontal plane is extended to the volumes bordered by both instrument beams and to the corresponding field of suspended sediment. The difference in the backscattering power at the two frequencies is related to the grain size–wave number product (Eq. 8) of an homogenous suspension and should not be influenced by the ensonifying of different water volumes. In a large river such as the Parana, the main gradients of the velocity and concentration fields take place over distances that are an order of magnitude larger than the typical measurements of the ensonified volume (fixed by the diverging beams and ADCP profiling resolution). This peculiarity of the Parana River yields the satisfactory calibration of the method over depth-time averaged samples. Nevertheless, the recordings at fixed positions showed noticeable variations with relatively short time periods (Figs. 4 and 6). These variations contained detailed patterns. Furthermore, beam divergence increases along the emission direction, which decreases the method reliability near the river-bed. Additionally, side lobe interference, which is also related to the beam angle (i.e. diverging beam), plays an important role near the bed. For these reasons, working with two adjacent, vertical beams of different frequencies may considerably improve the presented method. Indeed, three diverging beams are needed for velocity vector assessments, whereas the additional vertical beams could provide the layer homogeneity check and the complementary frequencies. In these regards, producing beam direction by means of phased array technology (Urick 1997), i.e. beam steering, may also be considered, so that the beam directions could be dynamically changed by introducing the appropriate phase delays depending on the ping purpose (velocity or concentration–grain size investigations).

Also the signal modulation operated by the ADCP reduces the method accuracy. In fact, this modulation is fixed in relation to the Doppler signal processing for flow velocity profiling (Gordon 1996). Given a flow velocity and its measurement accuracy, the modulated signal length increases with decreasing carrying frequency (i.e. acoustic frequency), which normally leads to larger bins and a greater distance to the first bin for lower-frequency ADCPs. In other words, with the objective of accurately assessing the backscattering power, the cell sizes for different frequencies could be made the same, which would also reduce the difference between first cell distances.

Another relevant limitation of the method is related to the frequency-dependent sensitivity of the acoustic transducer to suspended particles, which sets the acoustically inferred range of grain size. Indeed, the grain size is not unequivocally correlated to the backscattering power when the wave number–particle radius product, *ka*, is greater than 1. A *ka* value greater than 1 is beyond the Rayleigh scatter (Medwin and Clay 1998), and this sets the largest particle. On the other end of the spectrum, extremely fine sediment with a *ka* value less than 1 does not present scattering size ambiguities; however, the scattering power may be too low to be detected above the background noise threshold. This was assumed for sediment fractions finer than 80 μm in this study. Faults in Fig. 7b in individual bins mostly corresponded to the fine-sediment areas in Fig. 9. This correlation provides information regarding the results for a *ka* value that is too low for detection by 600 kHz. A higher frequency would help to fully investigate fine sediment within the observed streamflow core (0–400 m and 12–8 m as the transect distance and water depth, respectively, in Figs. 7–10). The assumed range for *ka* was 0.14–0.90, which corresponded to a detectable and measurable grain size range of 80–500 μm (the measured range in Fig. 2) for the applied frequencies. Given the same low threshold for *ka,* a 2000-kHz frequency may extend the range to 40 μm. In addition to this frequency-dependent limitation, the sound losses increase with frequency (Urick 1997), which would also affect the method capability of sizing finer sediment, particularly for long ranges and with high concentrations (Guerrero and Ruther 2013).

Regarding the performed calibration between the modelled backscattering power and averaged echo intensity, 60 and 95% confidence levels corresponded to bounds of 10–15 and 40–50%, respectively, of the actual predicted backscattering power ($S_v - S_c$ lines in Fig. 5) for the 1200- and 600-kHz ADCPs. Although more samples would be required to lower these uncertainties, in the case study, the slope coefficients (K_c) also corresponded to instrument conversion factors that were obtained in the laboratory, following the RD Instrument's technical note (1999). This observation confirmed the reliability of the applied model (Eq. 10) to predict the actual backscattering power by using depth-time averaged sampling in the Parana River. In fact, as demonstrated in Guerrero *et al.* (2012), instrument conversion factors can be applied for suspended sediment sizing. Calibration uncertainty is thus reduced to the intercept coefficient (C) uncertainty (reflecting the field variability of the background noise, E_r), which yields reduced bounds equal to 5–10 and 15–25% of the actual prediction for the 60 and 95% confidence levels, respectively.

A sediment sampler capable of collecting samples at specified depths may improve the calibration performance. The laser diffraction principle is applied (Sequoia Scientific 2010) to actual field measurements of concentration and grain size, achieving a time resolution similar to that of ADCP profiling. These techniques provide several data sets to match the ADCP record but may introduce bias because of the inaccurate depth alignment of point sampler measurements along the echo intensity profile and because of time misalignment between ADCPs measurements and concurrent measurement. The extent of these deviations should be considered with regards to observed vertical gradients and time variations (Guerrero and Ruther 2013).

Notwithstanding the aforementioned limitations, which explain the reported deviations in Table 3 and the method faults in Fig. 7b, the use of two ADCPs working at different frequencies demonstrates a high potential for river process investigations because of its capability to simultaneously map flow velocity, concentration and grain size distributions with good resolution. The method accounts for scattering power variation due to changes in the mean particle size in the ensonified volume. The observed variation of sediment concentration and size yielded the 20 and 30% variations, respectively, of the modelled scattering power over its average value. Using only one frequency, the grain size variation would lead to a lower accuracy of the method, which in this case, can be recast as a simplified relation between measured echo intensity and concentration. When applying single- or multi-frequency methods, the acoustic models applicability should be analysed in relation to the expected sediment concentration and grain size. Although the single-frequency method may be accurate enough for concentration assessments of well-sorted sediment, the multi-frequency method can be calibrated over a range of grain sizes. A changing size of the investigated sediment would imply different calibration coefficients to maintain the same accuracy by means of a single frequency. Furthermore, the limitations of the method depend on acoustic frequency in similar way as for single- and multi-frequency applications, which, by using 1200- and 600-kHz frequencies as in this Parana case study, led to a lower threshold of 80 μm for suspended sediment sizing.

The measurements collected at the Parana River cross-section provided evidence on two different mechanisms: (1) for coarse sediment, the entrapment from the bed into the stream flow by means of vertical advection in secondary currents (maximum concentration and grain size from 300 to 1200 m in Figs. 8 and 9, respectively) and (2) the observed transport of fine sediment within the core of the main streamflow (progressively from 0 to 300 m in Figs. 8 and 9). These results are in good agreement with the observed inertial effect in expansion–difluence units at the Parana River used to explain the loss of correlation between the flow velocity and sediment transport, as described by Szupiany *et al.* (2012). The observed variability at fixed positions provided detailed evidence on this sediment dynamics. The vertical velocity direction appeared to be correlated with a re-suspension-plume structure (concentration and grain size maps in Fig. 6) at low depths (P2 and P3 positions), whereas at the high-depth position, P4, the concentration and the flow velocity magnitude patterns appeared to be correlated.

These detailed results are not available from previous studies using the single-frequency method, and clarify the results of the first application on the Parana River of the dual ADCPs method, presented in Guerrero *et al.* (2011). The validation with depth-integrated samples yielded a reliable grain size distribution within the measurable range, whereas Guerrero *et al.* (2011) presented tentative distributions on the basis of known concentration values from a single-frequency application and an assumed univocal value of sediment mean grain size.

5 Conclusions

Our sampling effort on the Parana River validated the method for grain size assessment using two ADCPs working at different frequencies (600 and 1200 kHz) on the same water column. Good agreement was observed between the vertically integrated samples and the ADCPs-inferred results averaged over the depth and sampling time; the resulting squared correlation coefficients ranged from 0.5 to 0.9, and the obtained deviations from the samples were within 30 and 6% for the entire sample set and for the corresponding averages at fixed positions, respectively.

The flow velocity field, the concentration and grain size of the suspended sediments were extensively investigated in fixed positions and along the river cross-section, providing information on re-suspension-plume events from the river-bed. The coarse sediment (150–200 μm) of the measurable range was observed with maximum concentrations near the bed and in vertically stretched patterns. The time series at the fixed positions were characterized with re-suspension events correlated with the oscillations of flow velocity in the vertical direction. Plume and flow velocity variations showed 100–150 s periodicities and increasing magnitude

when passing from the channel thalweg to near low-depth areas of the bar. Suspended sediments with a grain size of approximately 100 μm were observed in full suspension within the streamflow core at the thalweg location.

Misalignment of acoustic beams and limited sensitivity to suspended particles restricted the applicability of the proposed method. Notwithstanding, the use of two ADCPs working at different frequencies showed a high potential for investigating large river processes because of the capability to simultaneously map flow velocity, concentration and grain size distributions with good resolution.

Acknowledgements

The authors would like to gratefully acknowledge the help provided by Roberto Viejo Mir and Santiago Cañete during the field measurements.

Funding

This research received funding from the European Community's Seventh Framework Programme (FP7/2007-2013) under Grant Agreement No. 212492 (CLARIS LPB. A Europe–South America Network for Climate Change Assessment and Impact Studies in La Plata Basin). This study was also conducted within the framework of the project "Analysis of construction processes in the floodplain of a large river: the Rio Paraná in its middle reach" granted by the Universidad Nacional del Litoral (Santa Fe, Argentina).

Notation

a	=	particle radius (m)
α	=	sound absorption coefficient in dB/m
C	=	calibration coefficient in dB
E	=	ADCP-measured echo intensity (counts)
E_r	=	echo intensity corresponding to the ambient noise level (counts)
f	=	particle form factor
k	=	acoustic wave number
K_c	=	conversion–calibration factor between the instrumental counts and dB
L	=	10 times the common logarithmic of the transmitted pulse length (m)
M	=	sediment concentration (kg m^{-3})
P	=	10 times the common logarithmic of the transmitted power (W)
R	=	acoustic beam range (m)
RL	=	received echo level (dB)
ρ_s	=	particle density (kg m^{-3})
s	=	backscattering power for unit volume (m^2 m^{-3})
S_c	=	backscattering power correction (dB)
SL	=	source level (dB)
S_v	=	backscattering power for unit volume (dB)
σ	=	scattering size (m^2)
T	=	transducer temperature (°C)
t	=	averaging time
TL	=	transmission loss (dB)
TS	=	target strength (dB)

References

Creed, E.L., Pence, A.M., Rankin, K.L. (2001). Inter-comparison of turbidity and sediment concentration measurement from an ADP, an ABS-3, and a LISST. Proc. Int. Conf. *Oceans 2001 MTS/IEEE*, Honolulu, (3) 1750–1754, Oceans 2000 MTS/IEEE Conference Committee and Marine Technology Society, Washington, DC and IEEE, Piscataway, NJ.

Deines, K.L. (1999). Backscattering estimation using broadband acoustic Doppler current profilers. Proc. Int. Conf. *IEEE sixth working conference on current measurement*, San Diego, S.P. Anderson, ed. IEEE, San Diego, CA, 249–253.

Drago, E., Amsler, M.L. (1998). Bed sediment characteristics in the Paraná and Paraguay rivers. *Water Int*. 23, 174–183.

Filizola, N., Guyot, J.L. (2004). The use of Doppler technology for suspended sediment discharge determination in the River Amazon. *Hydrol. Sci. J.* 49(1), 143–153.

Garcia M. 2008, Sedimentation Engineering: Processes Measurement, Modelling and Practice, ASCE Manuals and Report No. 110, ASCE Publications, Reston, Virginia, USA.

Gordon, R.L. (1996). *Acoustic Doppler current profilers: Principles of operation, a practical primer, second edition for broadband ADCPs. User manual*. Teledyne-RDI, San Diego, CA.

Guerrero, M., Di Federico, V., Lamberti, A. (2013). Calibration of a 2-D morphodynamic model using water–sediment flux maps derived from an ADCP recording. *J. Hydroinform*. 15(3), 813–828. doi:10.2166/hydro.2012.126

Guerrero, M., Lamberti, A. (2008). Field measurements of suspended sediment transport with acoustic multi frequencies technique. Proc. Int. Conf. *River flow 2008*, Cesme-Izmir, Turkey, (3) 2335–2341, M.S. Altinakar, M.A. Kokpinar, I. Aydin, S. cokgor, S. Kirkgoz, eds. Kubaba, Ankara.

Guerrero, M., Lamberti, A. (2011). Flow field and morphology mapping using ADCP and multibeam techniques: Survey in the Po River. *ASCE J. Hydraulic Eng.* 137(12), 1576–1587.

Guerrero, M., Ruther, N. (in press). On the possibility of using light scattering to validate multi-frequency ADCPs for investigating suspended sediment in rivers. *Flow Meas. Instrument*.

Guerrero, M., Ruther, N., Szupiany, R.N. (2012). Laboratory validation of ADCP techniques for suspended sediments investigation. *Flow Meas. Instrument* 23(1), 40–48.

Guerrero, M., Szupiany, R.N., Amsler, M. (2011). Comparison of acoustic backscattering techniques for suspended

sediments investigation. *Flow Meas. Instrument* 22(5), 392–401.

Hanes, D.M. (2012). On the possibility of single-frequency acoustic measurement of sand and clay concentration in uniform suspensions. *Cont. Shelf Res.* 46, 64–66.

Hay, A.E. (1983). On the remote acoustic detection of suspended sediment at long wavelengths. *J. Geophys. Res.* 88 (C12), 7525–7542.

Hay, A.E., Sheng, J. (1992). Vertical profiles of suspended sand concentration and size from multifrequency acoustic backscatter. *J. Geophys. Res.* 97(C10), 15661–15677.

Hoitink, A.J.F., Hoekstra, P. (2005). Observation of suspended sediment from ADCP and OBS measurements in a mud-dominated environment. *Coastal Eng.* 52 (2), 103–118.

Holdaway, G.P., Thorne, P.D., Flatt, D., Jones, S.E., Prandle, D. (1999). Comparison between ADCP and transmissometer measurement of suspended sediment concentration. *Cont. Shelf Res.* 19, 421–441.

Kostaschuk, R., Best, J., Villard, P., Peakall, J., Franklin, M. (2005). Measurement flow velocity and sediment transport with an acoustic Doppler current profiler. *Geomorphology* 68, 25–37.

Latrubesse, E. (2008). Patterns of anabranching channels: The ultimate end-member adjustments of mega rivers. *Geomorphology* 101, 130–145.

Mangini, S.P., Prendes, H.H., Amsler, M.L., Huespe, J. (2003). Importancia de la floculación en la sedimentación de la carga de lavado en ambientes del Río Paraná. *Revista Ingenieria Hidráulica En México*, 18(3), 55–56.

Medwin, H., Clay, C.S. (1998). *Fundamentals of acoustical oceanography*. Academic Press, London.

Muste, M., Yu, K., Pratt, T.C., Abraham, D. (2004a). Practical aspects of ADCP data use for quantification of mean river flow characteristics. Part II: Fixed-vessel measurements. *Flow Meas. Instrument.* 15(1), 17–28.

Muste, M., Yu, K., Spasojevic, M. (2004b). Practical aspects of ADCP data use for quantification of mean river flow characteristics. Part I: Moving-vessel measurements. *Flow Meas. Instrument.* 15(1), 1–16.

Oberg, K.A., Morlock, S.E., Caldwell, W.S. (2005). Quality assurance plan for discharge measurements using acoustic Doppler current profiles. *USGS scientific investigations report, 2005-5183*. U.S. Geological Survey, Washington, DC.

RD Instruments. (1999). Using the 305A4205 hydrophone to identify the RSSI scale factors for calibrating the echo strength output of an ADCP. *Technical note*. Teledyne-RDI, San Diego, CA.

Sequoia Scientific. (2010). *LISST-SL Version 2.1. User manual*. Sequoia Scientific, Inc., Bellevue, WA.

Szupiany, R.N., Amsler, M.L., Best, J.L., Parsons, D.R. (2007a). Comparison of fixed and moving vessel flow measurements with an aDp in a large river. *J. Hydraulic Eng.* 133(12), 1299–1309.

Szupiany, R.N., Amsler, M.L., Garcia, C.M. (2007b). Calibration of an ADP to estimate suspended sand concentrations in a large river. Proc. Int. Conf. *Hydraulic measurements & experimental methods 2007*, Lake Placid, NY, eds. EWRI and ASCE.

Szupiany, R.N., Amsler, M.L., Parsons, D.R., Best, J.L. (2009). Morphology, flow structure, and suspended bed sediment transport at two large braid-bar confluences. *Water Resour. Res.* 45, W05415.

Szupiany, R.N., Amsler, M.L., Hernandez, J., Parsons, D.R., Best, J.L., Fornari, E., Trento, A. (2012). Flow fields, bed shear stresses and suspended bed sediment dynamics in bifurcations of a large river. *Water Resour. Res*. 48, W11515.

Thorne, P.D., Hanes, D.M. (2002). A review of acoustic measurement of small-scale sediment processes. *Cont. Shelf Res.* 22, 603–632.

Thorne, P.D., Hardcastle, P.J. (1997). Acoustic measurement of suspended sediments in turbulent currents and comparison with in-situ samples. *J. Acoust. Soc. Am*. 101(5), 2603–2614.

Urick, R.J. (1948). The absorption of sound in suspensions of irregular particles. *J. Acoust. Soc. Am*. 20(3), 283–289.

Urick, R.J. (1997). *Principles of underwater sound*. Peninsula Publishing, Los Altos, CA.